Resolving glass transition in Te-based phase-change materials by modulated differential scanning calorimetry

OPEN ACCESS

Applied Physics Express **10**, 105601 (2017)

https://doi.org/**10.7567/APEX.10.105601**

Resolving glass transition in Te-based phase-change materials by modulated differential scanning calorimetry

Yimin Chen[1,2,3], Sen Mu[1], Guoxiang Wang[1], Xiang Shen[1*], Junqiang Wang[2*], Shixun Dai[1], Tiefeng Xu[1,2], Qiuhua Nie[1], and Rongping Wang[1]

[1]*Laboratory of Infrared Material and Devices & Key Laboratory of Photoelectric Materials and Devices of Zhejiang Province, Advanced Technology Research Institute, Ningbo 315211, China*

[2]*Key Laboratory of Magnetic Materials and Devices & Zhejiang Province Key Laboratory of Magnetic Materials and Application Technology, Ningbo Institute of Materials Technology & Engineering, Chinese of Sciences, Ningbo 315201, China*

[3]*University of Chinese Academy of Sciences, Beijing 100049, China*

*E-mail: shenxiang@nbu.edu.cn; jqwang@nimte.ac.cn

Received July 11, 2017; accepted September 11, 2017; published online September 26, 2017

Glass transitions of Te-based phase-change materials (PCMs) were studied by modulated differential scanning calorimetry. It was found that both $Ge_2Sb_2Te_5$ and GeTe are marginal glass formers with ΔT ($= T_x - T_g$) less than 2.1 °C when the heating rate is below 3 °C min^{-1}. The fragilities of $Ge_2Sb_2Te_5$ and GeTe can be estimated as 46.0 and 39.7, respectively, around the glass transition temperature, implying that a fragile-to-strong transition would be presented in such Te-based PCMs. The above results provide direct experimental evidence to support the investigation of crystallization kinetics in supercooled liquid PCMs. © 2017 The Japan Society of Applied Physics

Phase-change materials (PCMs) are commonly used in rewritable optical memory and/or electronic non-volatile devices owing to the reversible transition from the amorphous (high resistivity and low reflectivity) to crystalline phase (low resistivity and high reflectivity). Compared with the ongoing improvements in other memories, the data transfer speed of phase-change memory should be improved continuously.[1)] It is well known that understanding the crystallization kinetics of PCMs is necessary to improve their data transfer speed, and related topics have been widely investigated using various experimental tools and computer simulations.[2–5)] Nevertheless, a quantitative study of the crystallization kinetics in supercooled liquid requires the knowledge of fundamental thermal properties, such as peak crystallization temperature (T_p) and melting temperature (T_m), as well as glass transition temperature (T_g). Generally, T_p and T_m of PCMs are easily determined owing to a large enthalpy change in crystallization and melting processes. However, it is always challenging to obtain T_g experimentally because of the weak glass transition behavior, which is usually overlapped by the strong crystallization and/or relaxation signal in PCMs.

Recently, various methods have been employed to investigate the crystallization kinetics for PCMs, such as ultrafast calorimetry,[2–4,6)] dynamic transmission electron microscopy,[7)] laser irradiation,[8,9)] and electrical pulse heating.[10)] A viscosity model, namely, the Mauro–Yue–Ellison–Gupta–Allan (MYEGA) model based on the temperature-dependent configurational entropy,[11)] has been developed to study the crystallization kinetics. There are three parameters in the MYEGA model, i.e., fragility (m), T_g, and viscosity at infinite temperature (η_∞). It has been reported that a convergence of η_∞ at the particular value of $10^{-2.93}$ Pa s[12)] has physical meaning in terms of the constraint theory description.[13)] Thus, the MYEGA model can be considered as a two-parameter model in which the determination of m would be strongly influenced by T_g. It has been reported that the parameters of the crystallization kinetics, such as fragility, viscosity, and crystal growth rate, cannot be accurately estimated owing to the uncertain T_g.[14)] Therefore, it is highly desired to determine T_g in order to study crystallization kinetics.

Numerical simulations have been used to estimate T_g in PCMs in the last two decades. For instance, a T_g of 400 °C was calculated for $Ge_2Sb_2Te_5$ (GST).[15)] Hudgens and Johnson claimed that GST has a T_g of 350 °C.[16)] Compared with the onset temperature of crystallization (T_x), which is ~150 °C for GST,[17,18)] these values of T_g seem to be overestimated, because the T_g of the material is always lower than its T_x. A model based on the correlation between T_g and the enthalpy of atomization was presented for estimating the T_g of a covalent amorphous material.[19)] It showed that T_g was 111 °C for GST, which seems reasonable. However, T_g was estimated as 228 °C for GeTe, which is higher than its T_x of ~180 °C.[20)] On the other hand, experimental results were also obtained to investigate the glass transition in PCMs. For instance, by impedance and calorimetry measurements, the T_g for GST was reported as ~100 °C.[21)] However, the signal-to-noise ratio of the data is not good enough to be considered as strong evidence. Kalb et al. tried to detect the T_g signal in some Te-based PCMs via conventional differential scanning calorimetry (DSC).[22)] Nevertheless, no thermal signal of T_g was observed in the temperature range below its T_x at the heating rate from 5 to 80 °C min^{-1}. In their subsequent study, however, an endothermic signal of T_g before T_x was found after prolonged relaxation.[23)] The result showed that T_g is ~10 °C less than the crystallization temperature when the heating rate is 40 °C min^{-1}. Obviously, the determination of T_g in PCMs is still ambiguous and controversial.

Kalb et al. indicated that the weak glass transition in PCMs would be overlapped by relaxation and/or crystallization.[22,23)] It also implies that the conventional DSC is not a good choice for detecting such an overlapped and complex transition directly. Modulated DSC (mDSC) is a new development of DSC in which a small sinusoidal modulation is superimposed on the linear temperature ramp. A discrete Fourier transform algorithm is applied to the resultant data to

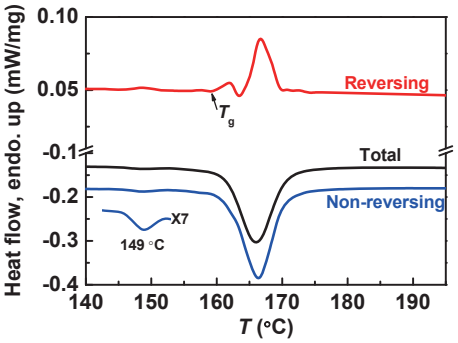

Fig. 1. Thermograms of amorphous GST showing a separation of glass transition and crystallization in the reversing (red) and nonreversing (blue) heat flow signals, respectively. The black line represents total heat flow, which is equal to the heat flow signal tested by conventional DSC. The linear heating rate is 3 °C min^{-1} and the sinusoidal modulation rate is 0.3 °C/1 min (the amplitude is 0.3 °C and the period is 1 min). The arrow indicates the glass transition temperature. The nonreversing thermogram between 142 to 153 °C was scaled to higher intensity in the left bottom to show the weak exothermic peak, and the scaling factor is given in the figure.

deconvolute the sample response to the underlying and modulated temperature programs.[24] This generates an output as "modulated heat flow", which can be separated into two components, i.e., reversing and nonreversing heat flows. Glass transition is a reversing component, but relaxation and crystallization are nonreversing components.[25] Therefore, mDSC can be utilized to separate the weak glass transition signal from the overlapped and complex heat flow.

In this work, we have investigated the glass transition in Te-based PCMs (GST and GeTe) using mDSC. It was found that T_g is very close to T_x in PCMs, and ΔT ($= T_x - T_g$) is smaller than 2.1 °C when the heating rate is below 3 °C min^{-1}, implying that they are marginal glass formers. Moreover, together with the conclusion of Kalb et al.,[23] a linear fitting can be applied to yield the GST and GeTe fragilities of 46.0 and 39.7, respectively, around T_g. The standard T_g values for GST and GeTe were also extrapolated as 167 and 187 °C, respectively.

Amorphous GST and GeTe films were deposited on SiO_2/Si(100) by magnetron sputtering using single GST and GeTe targets, respectively. For every deposition, the base and working pressures were set to $\sim 4 \times 10^{-4}$ and 0.35 Pa, respectively. The film thicknesses were 3 μm for GST and 2 μm for GeTe. The stoichiometry was confirmed by energy dispersive spectroscopy (EDS). Amorphous samples of 5 ± 1 mg weight were sealed in aluminum pans. Total, reversing, and nonreversing heat flow measurements were carried out using a NETZSCH instrument DSC204F1 calorimeter.

Figure 1 shows mDSC results for as-deposited GST, including total, reversing, and nonreversing heat flows. Apparently, no endothermic signal can be found in the total heat flow. However, by the specific function of separating an overlapped signal in mDSC, an obvious endothermic signal, which is ascribed to the glass transition, can be observed in the separated reversing heat flow. The corresponding onset temperature of the endothermic peak is determined to be 159.3 °C. The crystallization signal can be easily found in both total and nonreversing heat flows. It is more reasonable to estimate T_x at 161.7 °C from the nonreversing heat flow because the crystallization is a nonreversing process. Therefore, the parameter ΔT, which is defined as $T_x - T_g$, is only 2.4 °C for GST at a continuous heating rate of 3 °C min^{-1}. This implies that GST is a marginal glass former with a high crystallization speed. This is an important factor for screening a material that is useful for fast phase-change recording. In addition, a weak exothermic peak at ~149 °C is presented in the total and nonreversing heat flows. It can be observed clearly from the intensity-enhanced nonreversing heat flow in the left bottom in Fig. 1. This is ascribed to natural oxidization and results in the heterogeneous nucleation at the sample surface. It has been confirmed from the results of transmission electron microscopy that naturally oxidized Ge–Sb–Te alloys crystallize prior to the rest of the film.[18,26] Such weak crystallization behavior has also been reported by Kalb et al.[23] More interestingly, the endothermic signal in the reversing heat flow exhibits two peaks that are related to the amorphous structural evolution in a continuous heating process. The first endothermic peak is ascribed to the intrinsic signal of glass transition, while the second endothermic peak is due to the accompanying crystallization when the glass transition occurs simultaneously. This complicated process will be discussed in detail in future work.

We repeated the measurements and obtained similar results, confirming the reliability of the experiments. Such measurements were also carried out using other heating rates, i.e., 1 and 2 °C min^{-1}, and the results are shown in Figs. 2(a) and 2(b). The endothermic signal for glass transition can be observed in each reversing heat flow. The glass transition of GeTe was also studied by mDSC. As depicted in Figs. 2(c) and 2(d), T_g values for GeTe are 172 and 175.8 °C at heating rates of 1 and 2 °C min^{-1}, respectively. The corresponding characteristic temperatures with errors are listed in Table I.

Figure 3 shows the DSC traces for GST and GeTe at a heating rate of 40 °C min^{-1}. At such a high heating rate, the modulated model cannot reveal the weak glass transition in PCMs. Thus, here, we only employed the conventional model (linear heating) to detect the heat flow change during continuous heating. It can be seen that T_p is 180.1 and 200.8 °C for GST and GeTe, respectively. However, no endothermic signal of glass transition can be observed. For PCMs, Kalb et al. suggested that T_g at a heating rate of 40 °C min^{-1} can be determined as 10 °C below their T_p.[23] Therefore, the values of T_g at 40 °C min^{-1} for GST and GeTe can be inferred as 170.1 and 190.8 °C, respectively. Similar results were obtained in repeated measurements. Such characteristic temperatures with errors and corresponding calorimetric parameters are listed in Table I. As we can see, all the characteristic temperatures increase with the increase in heating rate. The parameter ΔT, which is a criterion to judge the glass forming ability, is only 1.8 and 2.1 °C for GeTe at heating rates of 1 and 2 °C min^{-1}, and 0.6 to 2.0 °C for GST when the heating rate increases from 1 to 3 °C min^{-1}. Such small ΔT indicates that these Te-based PCMs are marginal glass formers with a high crystallization speed, and thus are promising for fast phase-change memory. Moreover, the enthalpy changes that include the glass transition enthalpy ΔH_g and the crystallization enthalpy ΔH_c of GST and GeTe were calculated and the results are listed in Table I. It was found that ΔH_g increases with increasing heating rate, but ΔH_c remains almost constant for both GST and GeTe.

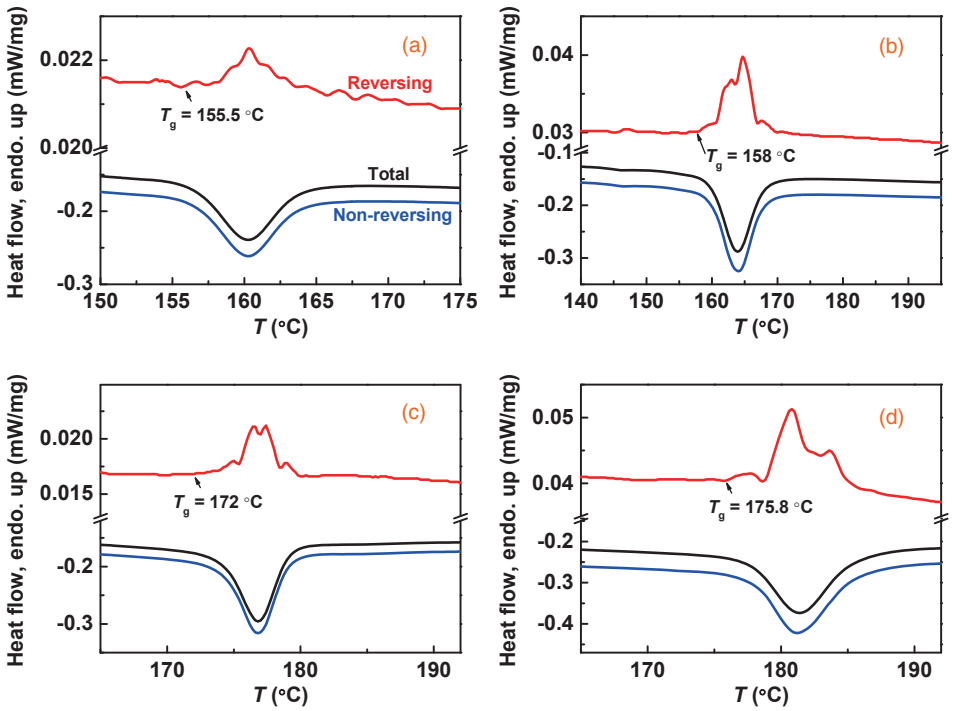

Fig. 2. Thermograms for amorphous GST at linear heating rates of (a) 1 and (b) 2 °C min^{-1}. Thermograms for amorphous GeTe at linear heating rates of (c) 1 and (d) 2 °C min^{-1}. The sinusoidal modulation rates are 0.18 and 0.3 °C/1 min when the linear heating rates are 1 and 2 °C min^{-1}, respectively. The arrows indicate glass transition temperatures.

Table I. Characteristic temperatures, ΔT, and enthalpy changes for GeTe and GST at different heating rates (ϕ in °C min^{-1}). The errors come from the repeated measurements.

	ϕ	T_x (°C)	T_p (°C)	T_g (°C)	ΔT (°C)	ΔH_g (J g^{-1})	ΔH_c (J g^{-1})
GeTe	1	174.2 ± 0.2	176.8 ± 0.1	172.4 ± 0.4	1.8	0.7 ± 0.21	−30.5 ± 1.1
	2	177.7 ± 0.2	181.4 ± 0.3	175.6 ± 0.5	2.1	0.9 ± 0.32	−31.2 ± 0.6
	40	197.2 ± 0.3	201.0 ± 0.2	191.0 ± 0.2[a)]	6.2	—	—
GST	1	156.2 ± 0.4	160.4 ± 0.2	155.6 ± 0.1	0.6	0.4 ± 0.15	−23.5 ± 0.2
	2	159.4 ± 0.4	163.5 ± 0.5	158.0 ± 0.1	1.4	1.3 ± 0.02	−28.2 ± 4.4
	3	161.1 ± 0.6	165.8 ± 0.2	159.1 ± 0.3	2.0	3.4 ± 0.50	−25.6 ± 1.2
	40	176.3 ± 0.2	180.2 ± 0.1	170.2 ± 0.1[a)]	6.1	—	—

a) These temperatures were evaluated in accordance with Kalb et al.'s conclusion.[23)]

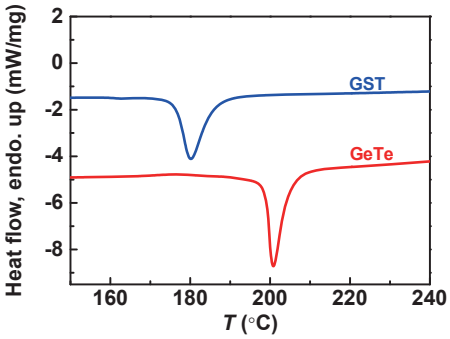

Fig. 3. DSC traces for GST and GeTe at a heating rate of 40 °C min^{-1}.

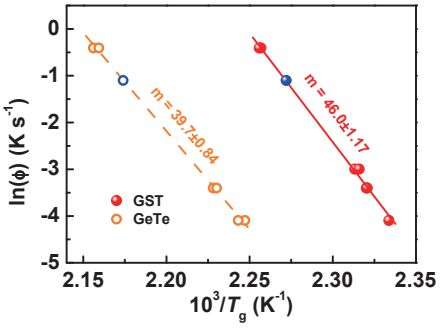

Fig. 4. Arrhenius plots for GST and GeTe. The red spheres and yellow circles represent the data of GST and GeTe, respectively. The red solid line and the yellow dashed line are the fitting results for GST and GeTe, respectively. The blue sphere and circle indicate the standard T_gs that were extrapolated from the Arrhenius plots.

We plotted $\ln\phi$ vs $1/T_g$ and the results are shown in Fig. 4. Note that the T_g at 40 °C min^{-1} was estimated by the method suggested by Kalb et al. Apparently, there is an excellent linear relationship with a good quality of fit ($R^2 > 0.996$) between $\ln\phi$ and $1/T_g$ for both GST and GeTe, implying that their conclusion strongly supports our experimental results. The fragility (m) can be obtained by determining the activation energy E_a at T_g and taking the slope of E_a/R. It yields $m = E_a/(\ln 10 \times T_g \times R)$, where T_g is the standard glass transition temperature that is determined at a heating rate of 20 °C min^{-1}. Note that the standard T_g cannot

be obtained directly here, but it can be extrapolated as 167 and 187 °C for GST and GeTe, respectively, using the Arrhenius plots. Thus, the fragility m can be estimated as 46.0 ± 1.17 and 39.7 ± 0.84 for GST and GeTe, respectively. However, on the basis of the ultrafast DSC, Orava et al. reported that m is ~90 for GST,[2] and our previous study showed m of GeTe of ~130.[27] Apparently, the present results of the fragility of PCMs are different from the previous ones. It may due to the fragile-to-strong transitions present in such Te-based supercooled liquids. A similar situation has been reported in Ag–In–Sb_2Te,[3] which exhibits an obvious fragile-to-strong transition with two kinds of temperature-dependent viscosity in the temperature range from T_g to T_m. The fragility m deduced from the weak dependence at low temperature from T_g to T_{fs} (the temperature of the fragile-to-strong transition) is 37,[3] while the fragility m' from the strong dependence at high temperature from T_{fs} to T_m is 135.[9] The fragile-to-strong transition magnitude (f), which is determined by $f = m/m'$,[28] can be estimated as 3.6 for the supercooled liquid Ag–In–Sb_2Te. Similarly, the supercooled liquids GST and GeTe may also show a fragile-to-strong transition, and the corresponding f values are 1.9 and 3.3, respectively. Such a high value of f is very beneficial for solving the dilemma of data retention at low temperature and crystallization speed at high temperature.

In summary, on the basis of mDSC, the weak glass transitions of PCMs (GST and GeTe) were successfully separated from crystallization. It was found that the T_g of PCMs is very close to T_x, resulting in ΔT of only 2.0 °C when the heating rate is 3 °C min^{-1} for GST and ΔT of 2.1 °C when the heating rate is 2 °C min^{-1} for GeTe. These results confirmed that such Te-based PCMs are marginal glass formers that are useful for ultrafast phase-change recording. Furthermore, Arrhenius plots of $\ln\phi$ vs $1/T_g$ yielded m values of 46.0 and 39.7 for GST and GeTe, respectively, around T_g. Compared with the previous reports, m at a high temperature range is larger than that in this work. This is attributed to the unrevealed fragile-to-strong transition in supercooled liquid GST and GeTe, and we estimated that the transition magnitudes f are 1.9 and 3.3 for GST and GeTe, respectively.

Acknowledgments This work was financially supported by the Natural Science Foundation of China (Grant Nos. 61377061, 61604083, and 11504931), the Public Project of Zhejiang Province (Grant No. 2014C31146), the Natural Science Foundation of Zhejiang Province (Grant No. LQ15F040002), the Natural Science Foundation of Ningbo City (Grant No. 2017A610094), and the One Hundred Talents Program of the Chinese Academy of Sciences. It is also sponsored by the K. C. Wong Magna Fund of Ningbo University.

1) I. Friedrich, V. Weidenhof, W. Njoroge, P. Franz, and M. Wuttig, J. Appl. Phys. **87**, 4130 (2000).
2) J. Orava, A. L. Greer, B. Gholipour, D. W. Hewak, and C. E. Smith, Nat. Mater. **11**, 279 (2012).
3) J. Orava, D. W. Hewak, and A. L. Greer, Adv. Funct. Mater. **25**, 4851 (2015).
4) B. Chen, J. Momand, P. A. Vermeulen, and B. J. Kooi, Cryst. Growth Des. **16**, 242 (2016).
5) G. C. Sosso, G. Miceli, S. Caravati, F. Giberti, J. Behler, and M. Bernasconi, J. Phys. Chem. Lett. **4**, 4241 (2013).
6) B. Chen, G. H. Brink, G. Palasantzas, and B. J. Kooi, J. Phys. Chem. C **121**, 8569 (2017).
7) M. K. Santala, B. W. Reed, S. Raoux, T. Topuria, T. LaGrange, and G. H. Campbell, Appl. Phys. Lett. **102**, 174105 (2013).
8) G. Eising, T. Damme, and B. J. Kooi, Cryst. Growth Des. **14**, 3392 (2014).
9) M. Salinga, E. Carria, A. Kaldenbach, M. Bornhofft, J. Benke, J. Mayer, and M. Wuttig, Nat. Commun. **4**, 2371 (2013).
10) A. Sebastian, M. Gallo, and D. Krebs, Nat. Commun. **5**, 4314 (2014).
11) J. C. Mauro, Y. Yue, A. J. Ellison, P. K. Gupta, and D. C. Allan, Proc. Natl. Acad. Sci. U.S.A. **106**, 19780 (2009).
12) Q. Zheng and J. C. Mauro, J. Am. Ceram. Soc. **100**, 6 (2017).
13) Q. Zheng, J. C. Mauro, A. J. Ellison, M. Potuzak, and Y. Yue, Phys. Rev. B **83**, 212202 (2011).
14) G. C. Sosso, J. Behler, and M. Bernasconi, Phys. Status Solidi B **249**, 1880 (2012).
15) C. Peng, L. Cheng, and M. Mansuripur, J. Appl. Phys. **82**, 4183 (1997).
16) S. Hudgens and B. Johnson, MRS Bull. **29**, 829 (2004).
17) J. Feng, Y. Zhang, B. W. Qiao, Y. F. Lai, Y. Y. Lin, B. C. Cai, T. A. Tang, and B. Chen, Appl. Phys. A **87**, 57 (2007).
18) T. H. Jeong, M. R. Kim, H. Seo, S. J. Kim, and S. Y. Kim, J. Appl. Phys. **86**, 774 (1999).
19) M. H. R. Lankhorst, J. Non-Cryst. Solids **297**, 210 (2002).
20) M. Libera and M. Chen, J. Appl. Phys. **73**, 2272 (1993).
21) E. Morales-Sánchez, E. F. Prokhorov, A. Mendoza-Galván, and J. González-Hernández, J. Appl. Phys. **91**, 697 (2002).
22) J. A. Kalb, F. Spaepen, and M. Wuttig, J. Appl. Phys. **93**, 2389 (2003).
23) J. A. Kalb, M. Wuttig, and F. Spaepen, J. Mater. Res. **22**, 748 (2007).
24) M. Reading, A. Luget, and R. Wilson, Thermochim. Acta **238**, 295 (1994).
25) N. J. Coleman and D. Q. Craig, Int. J. Phytoremediation **123**, 13 (1996).
26) J. A. Kalb, C. Y. Wen, F. Spaepen, H. Dieker, and M. Wuttig, J. Appl. Phys. **98**, 054902 (2005).
27) Y. M. Chen, G. X. Wang, L. J. Song, X. Shen, J. Q. Wang, J. T. Huo, R. P. Wang, T. F. Xu, S. X. Dai, and Q. H. Nie, Cryst. Growth Des. **17**, 3687 (2017).
28) C. Zhang, L. Hu, Y. Yue, and J. C. Mauro, J. Chem. Phys. **133**, 014508 (2010).